Dynamics of light particles in oscillating cellular flows

Roberto Festa,[1] Andrea Mazzino,[1,2] and Manuela Todini[1]

[1]*Department of Physics, University of Genova, via Dodecaneso 33, 16146 Genova, Italy*
[2]*INFN and CNISM, via Dodecaneso 33, 16146 Genova, Italy*

The dynamics of light particles in chaotic oscillating cellular flows is investigated both analytically and numerically by means of Monte Carlo simulations. At level of linear analysis (in the oscillation amplitude) we determined how the known fixed points relative to the stationary cellular flow deform into closed stable trajectories. Once the latter have been analytically determined, we numerically show that they possess the dynamical role of attracting all asymptotic trajectories for a wide range of parameters values. The robustness of the attracting trajectories is tested by adding a white-noise contribution to the particle equation of motion. As a result, attracting trajectories persist up to a critical Péclet number above which an average rising velocity sets in. Possible implications of our results on the long-standing problem related to the explanation of the observed oceanic plankton patchiness will be also discussed.

In this Rapid Communication we study the behavior of light particles in unsteady cellular flow fields. From a dynamical point of view, the flow time dependence is expected to produce dramatic effects on the particle dispersion. With regard to neutral particles (i.e., having the same density as that of the surrounding fluid) such effects have been clearly shown in [1] as a manifestation of resonance mechanisms eventually leading to anomalous transport [2,3].

Here, we do not focus on dispersion but rather on the rising process under gravity of particles having a density slightly smaller than that of the surrounding fluid (i.e., the counterpart of sedimentation occurring for particles having a density slightly larger than that of the surrounding fluid). For long enough time intervals, the rising process is the most effective transport mechanism, molecular and eddy diffusion being subleading due to the $t^{1/2}$ behavior of the variance of particle displacement. Why we consider this particular regime is motivated by two different reasons. First, the dynamics of particles slightly lighter than the surrounding fluid has attracted little attention, especially if compared with the limiting cases of heavy and very light (i.e., bubbles in water) particles. Second, this situation seems to be very attractive in the realm of oceanic sciences and ecology in connection to the understanding of phytoplankton distribution [4,5]. In many instances (the cyanobacteria is probably the best example) phytoplankton can indeed reduce its own original density by maintaining gas-filled space within the protoplast thus acquiring, in life, a positive buoyancy. For a review of mechanisms acting to reduce phytoplankton density we refer to [6].

Our main aims here are twofold. We will first investigate how chaos here induced by oscillations of cell position eventually alters the structure of the fixed points calculated in [7] for the static case (i.e., a time-independent cellular flow). The role of chaos on the spatial distribution of inertial particles has also been addressed in Ref. [8] with the goal of investigating autocatalytic reactions. The flow field considered there is however different from the one we will introduce in the sequel.

We will successively show how the resulting limit cycles (into which the static fixed points deform as a consequence of time dependence we introduced in the cellular flow) constitute a set of attracting trajectories where, after a transient time, all particles fall. This latter situation is associated to a vanishing particle mean rising velocity.

To start our analysis, let us consider the two-dimensional velocity field $\mathbf{u} \equiv (u_x, u_y)$ (in units of the velocity amplitude U)

$$u_x = \sin(x)\cos[y + B\sin(\omega t)],$$

$$u_y = -\cos(x)\sin[y + B\sin(\omega t)] \tag{1}$$

defined by the stream function

$$\psi(x,y) \equiv \sin(x)\sin[y + B\sin(\omega t)]. \tag{2}$$

This flow is a simple model for transport in time-periodic Rayleigh-Bénard convection [1,9] and Langmuir cells [10]. The stream function (2) describes a single-mode two-dimensional convection in squared cells of side 2π (in units of $L \equiv 1/k$, k being the cell wave number) with rigid boundary condition. The term $B\sin(\omega t)$ (times are in units of L/U) mimics possible oscillatory instabilities (e.g., the even oscillatory instability in Rayleigh-Bénard convection [11]) here represented in the form of vertical roll oscillations. The resulting flow field is thus intimately time dependent and exhibits Lagrangian chaos [12].

Our interest here is on the particle tracking under gravity of small spherical particles of radius a and mass m_p plugged into the flow field [Eq. (1)]. The resulting dynamical equations are [7,13]

$$m_p \frac{d\mathbf{V}}{dt} = (m_p - m_f)\mathbf{g} + m_f \frac{D\mathbf{u}}{Dt}(\mathbf{X}(t),t)$$

$$- \frac{1}{2}m_f \frac{d}{dt}\{\mathbf{V}(t) - \mathbf{u}(\mathbf{X}(t),t)\}$$

$$- 6\pi a\mu\{\mathbf{V}(t) - \mathbf{u}(\mathbf{X}(t),t)\}, \tag{3}$$

where $\mathbf{V}(t) \equiv \mathbf{V}(\mathbf{X}(t))$ is the particle velocity along its trajectory $\mathbf{X}(t)$, defined by the equation

$$\frac{d\mathbf{X}}{dt} = \mathbf{V}(\mathbf{X}(t)), \tag{4}$$

g is the gravitational acceleration, m_f is the mass of the displaced fluid, μ is the dynamic viscosity of the fluid, and the meaning of d/dt and D/Dt are the "particle" and "fluid"-associated Lagrangian derivatives, respectively. The coordinates x and y are aligned to the cells boundaries and gravity points along the negative y axis.

As customary, the particle velocity equation can be recast in dimensionless form upon introducing the Stokes number (St), the Froude number (Fr), and β as

$$\mathrm{St} \equiv \frac{U\tau}{L}, \quad \mathrm{Fr} \equiv \frac{U}{\sqrt{gL}}, \quad \beta \equiv \frac{3\rho_f}{2\rho_p + \rho_f},$$

where ρ_p and ρ_f are the particle density and fluid density, respectively. Finally, τ is the Stokes time, $\tau \equiv \rho_f a^2/(3\mu\beta)$. The parameter β ranges between 0 (heavy particle limit) and 3 corresponding to a vanishing particle density. The $\beta=1$ value corresponds to the neutral particle case [14,15].

In terms of the above dimensionless quantities, the particle equation of motion becomes

$$\frac{d\mathbf{V}}{dt} = \beta\frac{d\mathbf{u}}{dt}(\mathbf{X}(t),t) + \frac{(1-\beta)}{\mathrm{Fr}^2}\hat{\mathbf{g}} - \frac{[\mathbf{V}(t) - \mathbf{u}(\mathbf{X}(t),t)]}{\mathrm{St}}$$
$$+ \frac{2}{3}\beta[\mathbf{u}(\mathbf{X}(t),t) - \mathbf{V}(t)] \cdot \boldsymbol{\nabla}\mathbf{u}(\mathbf{X}(t),t). \tag{5}$$

We are now in the position to determine how the fixed points calculated in [7] for the static case $B=0$ [obtained by imposing the condition $d\mathbf{V}/dt=0$ in Eq. (5)] eventually deform into closed trajectories due to the effect of the vertical cell oscillation. The answer to this question is *a priori* not obvious owing to the chaoticity of the flow [Eq. (1)] whose mixing effects on the particle trajectories might destroy the structure of the fixed points.

Let us suppose that the cell oscillation (with amplitude B and pulsation ω) modifies the fixed points relative to the case $B=0$ in a way that the particle now performs a closed path around a given $B=0$ fixed point, rotating around it with the same flow pulsation ω. Whether or not the pulsation has to be equal to ω will be numerically verified *a posteriori*.

According to the above assumptions, let us take the following particle evolution:

$$X(t) = x_0 + a_x B\cos(\omega t) + b_x B\sin(\omega t),$$

$$Y(t) = y_0 + a_y B\cos(\omega t) + b_y B\sin(\omega t), \tag{6}$$

where (x_0, y_0) is the generic fixed point for the $B=0$ case [7].

In order to obtain the four unknown coefficients a_x, b_x, a_y, and b_y, we plug Eq. (6) into Eq. (5). Linearizing the resulting equation for small Bs (with respect to the cell size) and recalling that (x_0, y_0) satisfies the fixed point equation for $B=0$, the resulting equations read as

$$f_1 \cos(\omega t) + f_2 \sin(\omega t) = 0,$$

$$f_3 \cos(\omega t) + f_4 \sin(\omega t) = 0, \tag{7}$$

where f_1, f_2, f_3, and f_4 (all functions of a_x, b_x, a_y and b_y) are given by

$$f_1 = -\left[C + \mathrm{St}\omega^2 + \frac{2}{3}\beta\mathrm{St}\cos(2x_0)\right]a_x + Da_y$$
$$+ \omega\left[1 - \frac{1}{3}\beta\mathrm{St}C\right]b_x + \frac{1}{3}\omega\beta\mathrm{St}Db_y + \omega\beta\mathrm{St}D,$$

$$f_2 = -\omega\left[1 - \frac{1}{3}\beta\mathrm{St}C\right]a_x - \frac{1}{3}\omega\beta\mathrm{St}Da_y$$
$$- \left[C + \mathrm{St}\omega^2 + \frac{2}{3}\beta\mathrm{St}\cos(2x_0)\right]b_x + Db_y + D,$$

$$f_3 = -Da_x + \left[C - \mathrm{St}\omega^2 - \frac{2}{3}\beta\mathrm{St}\cos(2y_0)\right]a_y$$
$$- \frac{1}{3}\omega\beta\mathrm{St}Db_x + \omega\left[1 + \frac{1}{3}\beta\mathrm{St}C\right]b_y + \omega\beta\mathrm{St}C,$$

$$f_4 = \frac{1}{3}\omega\beta\mathrm{St}Da_x + -\omega\left[1 + \frac{1}{3}\beta\mathrm{St}C\right]a_y - Db_x + \left[C - \mathrm{St}\omega^2\right.$$
$$\left. - \frac{2}{3}\beta\mathrm{St}\cos(2y_0)\right]b_y + C - \frac{2}{3}\beta\mathrm{St}\cos(2y_0),$$

and we have defined $C \equiv \cos(x_0)\cos(y_0)$ and $D \equiv \sin(x_0)\sin(y_0)$.

By virtue of orthogonality of sine-cosine basis, system (7) leads to four nonhomogeneous linear equations for a_x, b_x, a_y, and b_y. Namely,

$$f_1(a_x, b_x, a_y, b_y) = 0,$$

$$f_2(a_x, b_x, a_y, b_y) = 0,$$

$$f_3(a_x, b_x, a_y, b_y) = 0,$$

$$f_4(a_x, b_x, a_y, b_y) = 0. \tag{8}$$

By simple algebra, the solution of the above linear system can be easily obtained. Its expression is quite lengthy and not particularly expressive. For these reasons it will not be reported here.

As announced in the introductory part, let us focus on the case of particles lighter than the surrounding fluid. Our choice for the parameter β is in the whole range $(1,3]$ although here, for the sake of brevity, we report and discuss the sole case $\beta=1.5$ (i.e., $\rho_f=2\rho_p$). The latter, for the static case, has been considered in [16]. For such value we know that the fixed points found in [7] are stable provided St is sufficiently small. For this reason we take St$=0.05$ whose value also ensures [13] the validity of approximations leading to the dynamical equation (5).

The analytical solution of Eq. (8) being now available, let us now pass both to verify its validity or accuracy and to
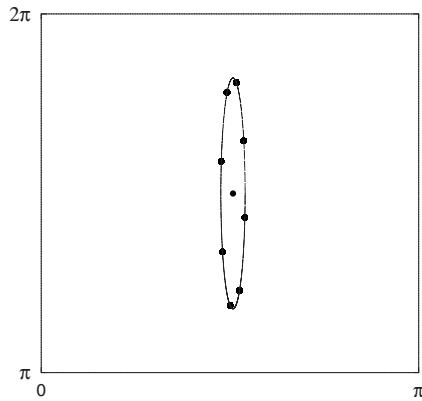
FIG. 1. Particle time evolution (the sampling time is 1/8 of the period of the orbit) from a Monte Carlo simulation (bullets) and the analytical trajectory obtained by solving Eq. (8) (continuous line). Parameters: $\omega=1$, St=0.05, $B=1$, Fr=1, and $\beta=1.5$. The bullet inside the closed trajectory is the static ($B=0$) fixed point.

address the question on whether or not the trajectories associated to the solution of Eq. (8) have a dynamical meaning. This latter issue is equivalent to ask whether such trajectories actually attract the long-time evolution of all particle trajectories. In order to answer these questions we have to resort to numerical simulations. The latter are performed by means of Monte Carlo simulations: we solve Eq. (5) by seeding the flow-field [Eq. (1)] by (up to) 10^6 particles. Time is advanced exploiting the Milstein's method [17] which easily permits to take into account white-noise contributions we will add later on the right-hand side (rhs) of Eq. (1).

The accuracy of the analytical trajectories having form (6) can be detected from Fig. 1. There, for a particle starting very close to the static (i.e., $B=0$ case) fixed point predicted in [7], we have reported (bullets) its time evolution and compared that with our analytical prediction (continuous line). The central bullet identifies the static fixed point. The agreement is good despite the value of order unity we used for B, close enough to that of the cell size. As far as the dependence in β is concerned, similar pictures are observed (not shown) for the whole $(1,3]$ β range and values of ω and St around
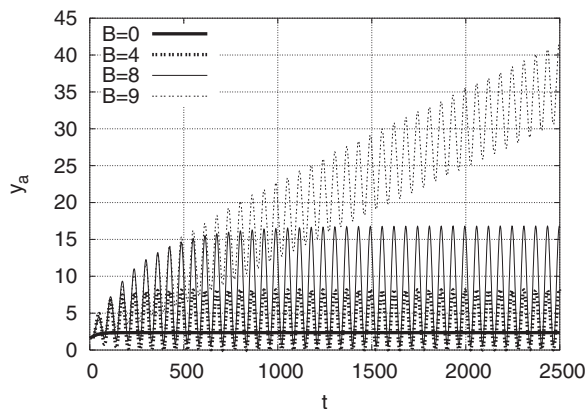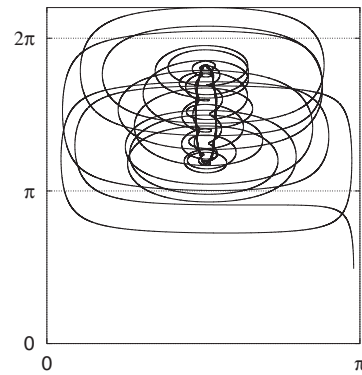

FIG. 3. Particle time evolution from a Monte Carlo simulation. Note how, after a transient, the particle falls on the analytically determined attracting trajectory. Parameters: $\omega=1$, St=0.05, $B=1$, Fr=1, and $\beta=1.5$.

those shown in the above picture. The way through which static fixed points deform thus seems sufficiently robust.

We are now in the position to answer the question on whether the trajectories around the static fixed points are attractors for the dynamics. To show that this is indeed the case, up to a critical value of B, we follow the dynamics of many particles (up to 10^6) and compute, at each time, the averaged vertical coordinate of our particles ensemble. Let us denote this time-dependent average by y_a. Its behavior is shown in Fig. 2 for different values of the cell oscillation amplitude. We can see the existence of a critical value for B, in between 8 and 9, separating the regime of nonrising particles ($B<8$) from that ($B>9$) where particles are observed to rise with a well-defined mean vertical velocity (in general different from the raising velocity in still fluid [18]). For B <8 we observed that all particles, after a transient, collapse on the attracting trajectories, which, at least for sufficiently small oscillation amplitudes, are well captured by our analytical expressions. We show in Fig. 3 this relaxation process for a given particle of the ensemble. With respect to Fig. 1, the only difference is in the initial position of the testing particle, here not necessarily in the vicinity of the static fixed point. For values of B larger than 9 the attracting trajectories
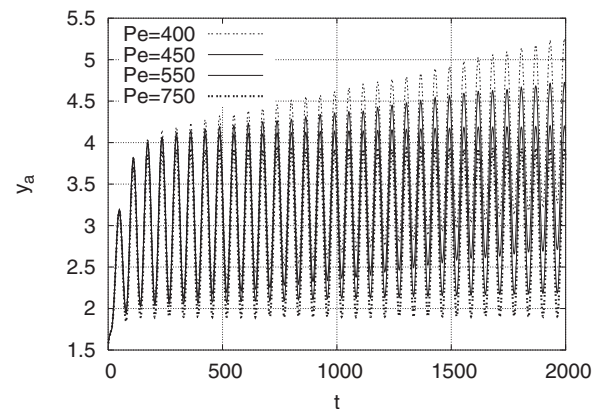

FIG. 2. The averaged vertical position of the particles ensemble as a function of time for four values of B. Parameters: $\omega=1$, St $=0.05$, Fr=1, and $\beta=1.5$. Note the crossover from a nonrising regime to a rising one for $B \in [8,9]$.

FIG. 4. The averaged vertical position of the particles ensemble as a function of time for four values of Pe. Parameters: $\omega=1$, St $=0.05$, Fr=1, $B=1$, and $\beta=1.5$. Note the crossover from a nonrising regime to a rising one occurring for Pe $\in [550,750]$.

go to breakdown. This appears as a result of a growing process of the attracting trajectories which become larger and larger as B increases until they reach the horizontal size of the cell. This happens just in between $B=8$ and $B=9$.

In order to check further the robustness of attracting trajectories we add on the rhs of Eq. (5) a white-noise contribution with coefficient $2/(\text{PeSt}^2)^{1/2}$, Pe being the Péclet number. Physically, this is a standard way to model Brownian contributions to the deterministic particle dynamics [18].

Our question is on whether even a small amount of randomness might destroy the emergence of attracting trajectories. From our Monte Carlo simulations this does not seem the case. In Fig. 4 we show the averaged vertical position of the particles ensemble as a function of time for different values of Pe. We note how, for $\text{Pe} \geq 750$ the averaged rising velocity remains zero. This phenomenon is still associated to the existence of attracting trajectories whose geometrical shape can be seen as a random perturbation of the attracting trajectories determined in the absence of noise. The single trajectory around the static fixed point found for the fully deterministic case is thus replaced by a patchiness particles distribution spread around the fixed point. As expected, attracting trajectories disappear for sufficiently large noise ($\text{Pe} < 750$ in our simulations).

Let us now conclude with some remarks emphasizing some possible implications of our results in applied contexts with a special emphasis to ecology. In this latter field, one of the long-standing problems is on the understanding of the very origin of plankton patchiness observed in the ocean in the form of persistent structures irrespective of the mixing induced by turbulent diffusion [19]. By means of a simple chaotic cellular flow field, we show both analytically and numerically the existence of attracting trajectories where particles lighter than the surrounding fluid asymptotically stay.

Such trajectories are found to exist irrespective of the mixing induced both by chaos and by molecular or eddy diffusion.

Our results thus seem to suggest that phytoplankton patchiness may have a dynamical explanation where the key ingredients are the smallness of density difference between fluid and phytoplankton, the light character of the phytoplankton and, finally, its inertia.

[1] P. Castiglione, A. Crisanti, A. Mazzino, M. Vergassola, and A. Vulpiani, J. Phys. A **31**, 7197 (1998).

[2] P. Castiglione, A. Mazzino, P. Muratore-Ginanneschi, and A. Vulpiani, Physica D **134**, 75 (1999).

[3] K. H. Andersen, P. Castiglione, A. Mazzino, and A. Vulpiani, Eur. Phys. J. B **18**, 447 (2000).

[4] M. A. Bees, Appl. Sci. Res. **59**, 141 (1997).

[5] T. Kolokolnikov, C. Ou, and Y. Yuan, J. Math. Biol. **59**, 105 (2009).

[6] C. S. Reynolds, *Ecology of Phytoplankton* (Cambridge University Press, Cambridge, England, 2006).

[7] M. R. Maxey, Phys. Fluids **30**, 1915 (1987).

[8] T. Nishikawa, Z. Toroczkai, C. Grebogi, and T. Tél, Phys. Rev. E **65**, 026216 (2002).

[9] T. H. Solomon and J. P. Gollub, Phys. Rev. A **38**, 6280 (1988).

[10] I. Langmuir, Science **87**, 119 (1938).

[11] R. M. Clever and F. H. Busse, J. Fluid Mech. **65**, 625 (1974).

[12] A. Crisanti, M. Falcioni, A. Vulpiani, and G. Paladin, Riv. Nuovo Cimento **14**, 1 (1991).

[13] M. R. Maxey and J. J. Riley, Phys. Fluids **26**, 883 (1983).

[14] A. Babiano, J. H. E. Cartwright, O. Piro, and A. Provenzale, Phys. Rev. Lett. **84**, 5764 (2000).

[15] P. Tallapragada and S. D. Ross, Phys. Rev. E **78**, 036308 (2008).

[16] C. Marchioli, M. Fantoni, and A. Soldati, Phys. Fluids **19**, 098101 (2007).

[17] P. E. Kloeden and E. Platen, *Applications of Mathematics (New York)* (Springer-Verlag, Berlin, 1992), Vol. 23.

[18] M. Martins Afonso, J. Phys. A: Math. Theor. **41**, 385501 (2008).

[19] T. J. Pedley and J. O. Kessler, Annu. Rev. Fluid Mech. **24**, 313 (1992).